Journal of Applied Fluid Mechanics, Vol. 18, No. 10, pp. 2518-2534, 2025.
Available online at www.jafmonline.net, ISSN 1735-3572, EISSN 1735-3645.
https://doi.org/10.47176/jafm.18.10.3419

Characterization of Lip Thickness Effects in Subsonic Coaxial Jets with Varying Velocity Ratio

I. Angelin[1], R. Naren Shankar[1], K. Sathish Kumar[2†], K. Anusindhiya[3], K. Vijayaraja[4], and E. Rathakrishnan[5]

[1] *Department of Aeronautical Engineering, Vel Tech Rangarajan Dr. Sagunthala R&D Institute of Science and Technology, Avadi, Tamil Nadu, 600062, India*
[2] *Department of Aeronautical Engineering, Nehru Institute of Engineering and Technology, Coimbatore, Tamil Nadu, 641105, India*
[3] *Department of Aeronautical Engineering, KIT – Kalaignarkarunanidhi Institute of Technology, Coimbatore, Tamil Nadu, 641402, India*
[4] *Department of Aeronautical and Aerospace Engineering, KCG College of Technology, Chennai, Tamil Nadu, 600097, India*
[5] *Department of Aerospace Engineering, Indian Institute of Technology - Kanpur, Kanpur, Uttar Pradesh, 208016, India*

†*Corresponding Author Email: nietdrksathishkumar@nehrucolleges.com*

ABSTRACT

This study aims to investigate the influence of lip thickness and velocity ratio on the mixing characteristics of coaxial jets. The primary objective is to examine and compare the flow behavior of thin and thick lip coaxial nozzles at various velocity ratios, using both experimental and numerical methods. The scope of the work focuses on identifying critical lip thicknesses ranging from 0.7 mm to 10.7 mm, in increments of 2 mm. The primary jet exit Mach number is maintained at 0.6, while the secondary jet Mach number is varied from 0% to 100% of the primary jet velocity. Numerical simulations are performed using a validated turbulence model to understand the flow physics, such as potential core variation and jet interaction mechanisms. In this research, the Reynolds number vary from 0 to 1.62×10^5 and the turbulence intensity has a minimum value for a 4 and it reaches to 4.9 at maximum. The results show that in thin lip nozzles, the increase in velocity ratio extends the potential core length due to dominant shear layer interaction. In contrast, thick lip nozzles display reduced core length with increasing velocity ratio, primarily due to wake region interaction. Among the cases studied, the 10.7 mm lip thickness configuration exhibits superior mixing characteristics, indicating the presence of a critical lip geometry for enhanced performance. These findings provide insight into optimizing coaxial jet design for applications requiring efficient mixing.

Article History

Received February 10, 2025
Revised May 7, 2025
Accepted May 11, 2025
Available online August 5, 2025

Keywords:

Thin lip
Thick lip
Velocity ratio
Shear dominant
Wake dominant

1. INTRODUCTION

In subsonic coaxial jets, the interaction between the primary and secondary flows leads to the formation of a complex flow structure in the near-field region. The geometry of the lip plays a significant role in determining the dominant flow behavior. A thin lip configuration promotes a shear-dominant flow, characterized by the development of two distinct shear layers: the primary mixing layer, between the primary and secondary jets, and the secondary mixing layer, between the secondary jet and the surrounding ambient fluid, as illustrated in Fig. 1(a). These shear layers interact and enhance the overall mixing effectiveness. In contrast, a thick lip induces a wake-dominant flow, where flow separation and wake formation downstream of the lip alter the mixing characteristics. The role of these shear layers in enhancing mixing has been previously reported by Ko and Kwan (1976).

In contrast, the wake-dominated flow exhibits a sub-atmospheric pressure region in the near field, as illustrated in Fig. 1(b). This low-pressure region induces an inward bending of the outer jet toward the inner jet axis, resulting in strong interaction between the inner and outer streams. Consequently, this interaction leads to a reduction in the primary jet core length (Orlu et al., 2008).

Several investigations have been conducted on low subsonic coaxial jets with both thin and thick lip configurations to gain a deeper understanding of the complex flow field behavior. Dahm et al. (1992) conducted experiments with a water coaxial jet with lip1.27mm, primary jet exit velocities of 0.1m/s to

Nomenclature

Symbols

D_p	primary nozzle exit diameter
k-ω	turbulent Kinetic Energy - Turbulent dissipation
M	freestream Mach number
M_e	exit Mach number
P_{ox}	local Axial Pressure
P_o	settling chamber total pressure
R	coordinate along the radial jet
RSM	Reynolds-Stress Model
SA	Spalart-Allmaras
SST	Shear-Stress Transport
U_p	primary jet exit velocity
U_s	secondary jet exit velocity
X	coordinate along the jet axis
γ	specific heat ratio

Definitions, Acronyms and Abbreviations

CDR	Characteristic Decay Region
CFD	Computational Fluid Dynamics
CFJ	Co-Flowing Jet with primary jet surrounded by secondary jet
FDR	Fully Developed Region
IMZ	Initial Merging Zone
IZ	Intermediate Zone
FMZ	Fully Merged Zone
PCF	Percentage Coaxial Jets
PCL	Potential Core Length
VR	Velocity Ratio

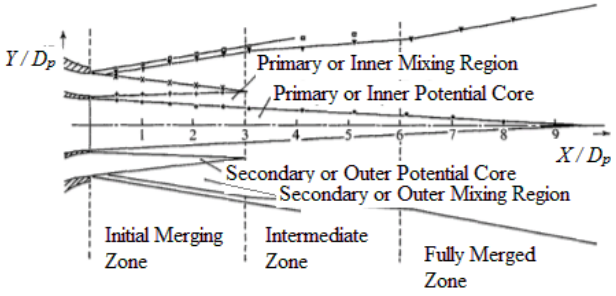

(a)

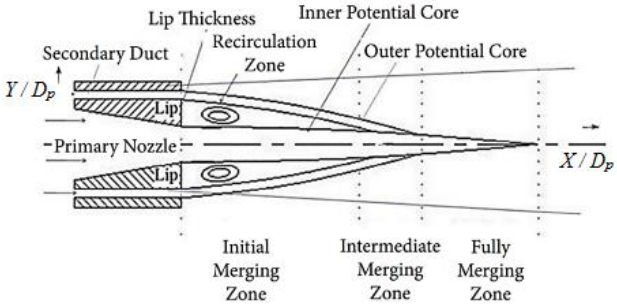

(b)

Fig. 1 Schematic representation of coaxial jets: (a) Thin lip (Ko & Kwan, 1976), (b) Thick lip (Naren Shankar et al., 2021)

0.25m/s, and velocity ratios ranging from 5.9 to 41.6 (percentage more than 100 indicates secondary jet has more velocity than primary jet). When the velocity ratio ([Secondary jet exit velocity (U_s) / Primary jet exit velocity (U_p)] is less than 1, the flow field can be clearly identified by three distinct regions: the initial merging region, the intermediate region, and the fully merged region. These regions represent the progressive mixing and interaction between the primary and secondary jets along the axial direction. However, when the velocity ratio (U_s/U_p) is greater than 1, the inner jet exit pressure is lower than the outer jet exit pressure, which makes the outer jet bend toward centreline and this bending becomes predominant with increasing velocity ratio.

Studies on thin lip coaxial jets show that when the velocity ratio is less than 100%, increasing the velocity ratio increases the potential core of the primary jet (Georgiadis & Papamoschou, 2003). In contrast when the velocity ratio is greater than 1, increasing the velocity ratio decreases the primary jet core length (Champagne & Wygnanski, 1971). Kwan and Ko (1976) by maintaining a constant secondary jet exit velocity of 50m/s and the primary jet exit velocity was varied from 1m/s to 6.67m/s, concluded that the outer core end is the extent of IMZ.

In thin lip coaxial jets, the shearing effect between the jets gives rise to the mixing enhancement whereas the wake/recirculation region will be negligible. In thick lip coaxial jets, mixing is due to the vigorous interaction between the primary and secondary jets, which is due to the wake region. Increasing the lip thickness from 2mm (Buresti et al., 1994) to 5mm (Segalini & Talamelli, 2011), 16mm (Chigier & Beer, 1964), increases the mixing in thick lip due to the frequency of vortex shedding.

Coaxial jets with mid lip fall between thick lip (around 10mm) and thin lip jets (around 1mm). Due to the middle range variation in the lip thickness, the coaxial jet becomes neither shear dominant nor wake dominant. This mid lip thickness does not predominantly inhibit/enhance mixing when the velocity ratio increases or decreases. (Srinivasarao et al., 2014a) studied a coaxial jet with a lip thickness of 1.5mm (thin lip) and 4.5mm (mid lip) and found enhanced mixing characteristics of the mid lip jet compared to a circular jet at subsonic Mach numbers of 0.6, 0.8 and 1.0. (Naren Shankar et al., 2020) showed that the mixing in coaxial jet (LT5mm, PCL of X/D_p = 3.16) is higher than the mixing from thin lip coaxial jets (LT2mm, PCL of X/D_p = 11.04).

In a study conducted by (Srinivasarao et al., 2014b), it was observed that the use of both thin lip thickness (1.5mm) and thick lip thickness(4.5mm) in a coaxial jet from an orifice, improve the mixing of the primary jet at various under-expanded conditions. Coaxial jets with a lip thickness of 0.4mm have superior mixing capabilities at low velocity ratio over the high velocity ratio due to the predominant mixing of the shear layer between the primary and secondary jets at different Mach numbers (M = 0.37, 0.6, 0.9) (Georgiadis & Papamoschou, 2003). A study done by (Inturi et al., 2022) found that the core length extended upto X/D_p=4 for a lip3mm having the primary jet exit diameter of 6mm with a 30 percentage co-

flowing jet. A study by (Hewes & Mydlarski, 2023) demonstrated the possible differences observed in the multiple combinations of primary jet exit gases and the mixing in co-flow jets at M >1 (M2.1,4.2) 0and M<1 (M0.77). They concluded that by limiting the analysis to a single velocity or a scalar field, different inferences would be drawn regarding the impact of the momentum flux ratio on the flow. Zaman and Dahl (2007) established that coaxial jets with a 0.762mm lip at subsonic Mach numbers possess high levels of noise as compared to a single equivalent jet.

From the literature, it is evident that the coaxial jets studied were for thick, moderate and thin lip thicknesses. These works focused mainly on random variations in lip thickness like 2mm to 10mm (Naren Shankar & Ganesan, 2022), 1.5mm to 4.5mm (Srinivasarao et al., 2014a), 2mm to 5mm (Orlu et al., 2006) so on and so forth. Also, the coaxial nozzles studied were not in a systematic lip thickness variation. A systematic variation of lip thickness from 2.65 mm to 10.7mm in terms of 2mm and with velocity ratio variation from 20% to 100% on the interval of 20% might play a dominant role in modifying the mixing characteristics of coaxial jets. To have a closer look at this important control parameter, thin, mid and thick lip subsonic jets issuing from coaxial nozzles with velocity ratios of 20%, 40%, 60%, 80% and 100% are studied quantitatively and qualitatively in this investigation. Also, the flow field in the coaxial jet in the XY plane was visualised using velocity contours to understand the effect of mixing and the shear layers in the near field of the jet.

Varying velocity ratios is essential for understanding coaxial jet mixing behavior and optimizing nozzle design for real-world applications. By altering the velocity ratio between the primary and secondary jets, this study examines the influence on shear layer and wake formation, total pressure variation, static pressure variation at the nozzle near field and potential core length. This knowledge is critical for applications such as jet noise reduction, thrust optimization in aerospace propulsion, and fuel-efficient combustion in gas turbines. Furthermore, varying design parameters like lip thickness, nozzle exit area, and nozzle geometry enables fine-tuning the jet characteristics to improve performance in practical engineering systems. Ultimately, this research contributes to advancements in innovative engineering solutions to enhance technology, benefit industries, and society.

Coaxial jets have a wide range of practical applications across various engineering fields. In aerospace, they are commonly used in turbofan engines to improve thrust and fuel efficiency. As a confined coflow system, coaxial jets are applied in dual-combustion ramjet (DCR) engines and in scramjet inlets, where the isolator serves as the primary flow path and the air entering the combustor functions as the secondary flow. Beyond aerospace, coaxial jets are also utilized in industrial systems such as welding torch nozzles and firefighting nozzles to enhance jet control and penetration. Additionally, they play an important role in thrust augmentation systems, mixing tanks, sludge agitation, and other fluid mixing applications. These jets are effective in promoting better mixing, improving efficiency, and enhancing performance in various flow-driven processes.

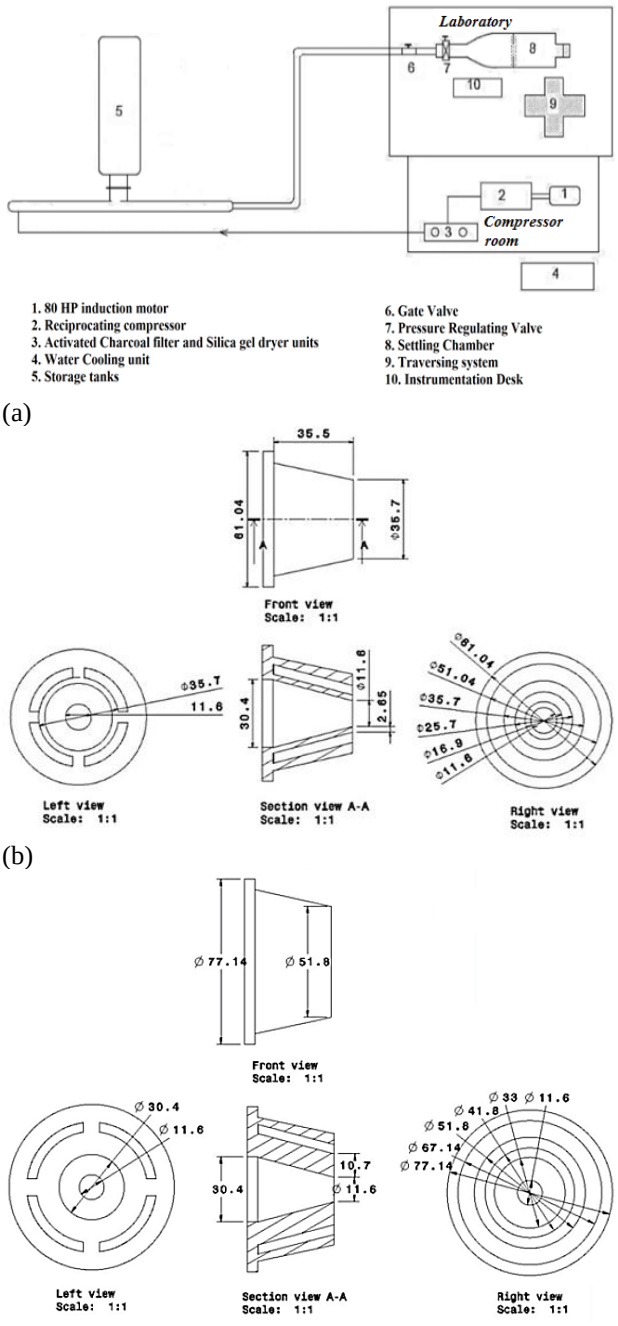

Fig. 2 (a) High speed jet facility, (b) Layout of thin lip coaxial nozzle LT2.65mm, (c) Layout of thick lip coaxial nozzle LT10.7mm

2. EXPERIMENTAL DETAILS

2.1 Jet Flow Facility

The experimental investigations were carried out in the coaxial jet test facility located at the High-Speed Aerodynamics Laboratory, Vel Tech Rangarajan Dr. Sagunthala R&D Institute of Science and Technology, Chennai, India (Fig. 2a). Compressed air from a high-pressure storage reservoir was regulated through a control valve and directed into the primary settling chamber, which feeds the primary nozzle. The secondary nozzle was

similarly supplied via an independent secondary settling chamber. The desired exit Mach numbers were achieved by precisely controlling the total (stagnation) pressure (p_o) in the respective settling chambers. Pressure conditions for both the primary and secondary jets were adjusted by setting appropriate back pressure levels, with reference to isentropic flow relations, to maintain the required operating Mach numbers at the nozzle exits.

2.2 Experimental Models

The experimental investigation utilized a series of coaxial nozzle configurations with lip thicknesses of 2.65 mm, 4.7 mm, 6.7 mm, 8.7 mm, and 10.7 mm. All nozzles featured a common primary nozzle exit diameter of 11.6 mm and a secondary nozzle exit width of 4.4 mm. The geometric configurations representing the thin and thick lip coaxial nozzles are illustrated in Figs 2(b) and 2(c), respectively.

2.3 Instrumentation

Pitot pressure variation along the axial direction of the jet and radial direction of the jet, at different axial locations, were measured with a WIKA sensor with a range of 0-10 bar. The accuracy of the transducer (after the re-zero calibration) is specified to be ±0.15% full scale. The total pressure measurement was done using a Pitot tube of 0.4mm and 0.6mm inner and outer diameters. The probe is mounted on a traverse mechanism with a resolution of 0.1mm in linear translation. Thus, the ratio of the primary nozzle exit diameter to the probe area is $((11.6)^2 / (0.6)^2) = 373.78$. The minimum secondary exit area will be there for a 2.65mm lip coaxial nozzle. For that nozzle the inner diameter is 16.9mm, the outer diameter is 25.7mm, and its area to the probe blockage area will be $((25.7)^2 - (16.9)^2 / (0.6)^2) = 1041.3$ which is well above the limit of 64 for neglecting the probe blockage effect (Rathakrishnan, 2009). In the present study, every measured Pitot pressure has an average value of 500 samples per second which are repeatable within ±3%.

3. Results And Discussions

3.1 Axial Pressure Variation

The axial variation or decay of Pitot pressure serves as an indicator of the mixing behavior between the primary and secondary jet streams, as well as with the ambient entrained fluid. To quantify this, the local axial pressure (P_{ox}) measured along the jet centerline is non-dimensionalized by the settling chamber total pressure (P_o) and plotted as a function of the non-dimensional axial distance (X/D_p), where D_p denotes the primary nozzle exit diameter.

The parameter P, representing the normalized centerline total pressure (P_{ox}/P_o) is calculated using the isentropic pressure relation (1):

$$\frac{P_o}{P_{ox}} = \left(1 + \frac{\gamma-1}{2} M^2\right)^{\frac{\gamma}{\gamma-1}} \quad (1)$$

The specific heat ratio $\gamma = 1.4$ is used for air, and the Mach number M considered in this study is 0.6.

The primary and secondary jet exit Mach numbers, along with their corresponding total pressures at the exit plane, are summarized in Table 1. Additionally, the table presents the velocity ratio (VR) expressed as a percentage of the primary jet velocity, the observed potential core lengths, and the relative elongation of the core with variation in velocity ratio and lip thickness. This comparative data provides insight into the influence of jet configuration on flow development and mixing efficiency.

In Fig. 3(a), the plot illustrates variations in velocity ratio compared to a LT0.7mm. When considering a single jet, the potential core length (PCL) is measured at 4.01. However, with a 0.7mm lip and VR20, the PCL extends to 4.96. This elongation in PCL is attributed to the coaxial phenomenon, which protects the mainstream from collaborating with the surrounding air. As the VR increases, this elongation intensifies, resulting in a potential core length of 6.99, 8.61, 9.84 and 10.5 for VR values of 40, 60, 80, and 100, respectively, as detailed in Table 1. Low velocity ratios correspond to increased shear effects, diminishing the core extent of the primary stream. Conversely, high velocity proportion indicate reduced shear effects but increased shielding, leading to an expanded core of the mainstream.

In the case of a 1.7mm lip thickness (depicted in Fig. 3b), the core extent ranges to $X/D_p = 4.57$ without coaxial jet, while with a coaxial jet, the core growths from $X/D_p = 5.16$ for VR20 to $X/D_p = 10.5$ for VR100 as the velocity ratio rises.

For lip2.65mm (Fig. 3c), the total pressure variation is shown for VR0, VR10, VR20, VR30, VR40, VR50, VR60, VR70, VR80, VR90, and VR100. Figure 3(a) has been compared with (Inturi et al., 2022) in order to observe the curve trend. The curve shows the centerline total pressure variation plot for M0.5 for 30PCFJ. It is observed that the results of the current study match the trend. For LT2.65mm it is seen that the jet core length increases with an increase in velocity ratio. For LT265mm, all LT2.65mm, VR20 has the shortest core followed by a rapid decay in Pitot pressure. The mixing of VR20 and VR40 jet are superior to that of the VR60, VR80 and VR100 jets in the core region as indicated by a shorter core. At low VR, the shearing effect is more. This increases the entrainment between the two jets thereby reducing the core. When VR increases, core length of the primary jet elongates. The shear layer causes the near field mixing, which is dominant at VR20 and VR40 jets. Furthermore, the mixing promotion caused by VR20 and VR40 jets are superior to that for VR60, VR80 and VR100 jets even in the characteristic decay region. For other lip thickness, the same trend is repeated.

For the lip thickness of 4.7 mm (Fig. 3d), the elongation of the potential core length (PCL) with increasing velocity ratio (VR) is comparatively less pronounced than that observed for the 2.65 mm lip configuration, as corroborated by data in Table 1. This behavior can be attributed to a combined influence of shear layer interaction and wake formation in the near-field mixing region. At this intermediate lip thickness, the competing effects of shear-dominated and wake-dominated mixing tend to counterbalance each other,

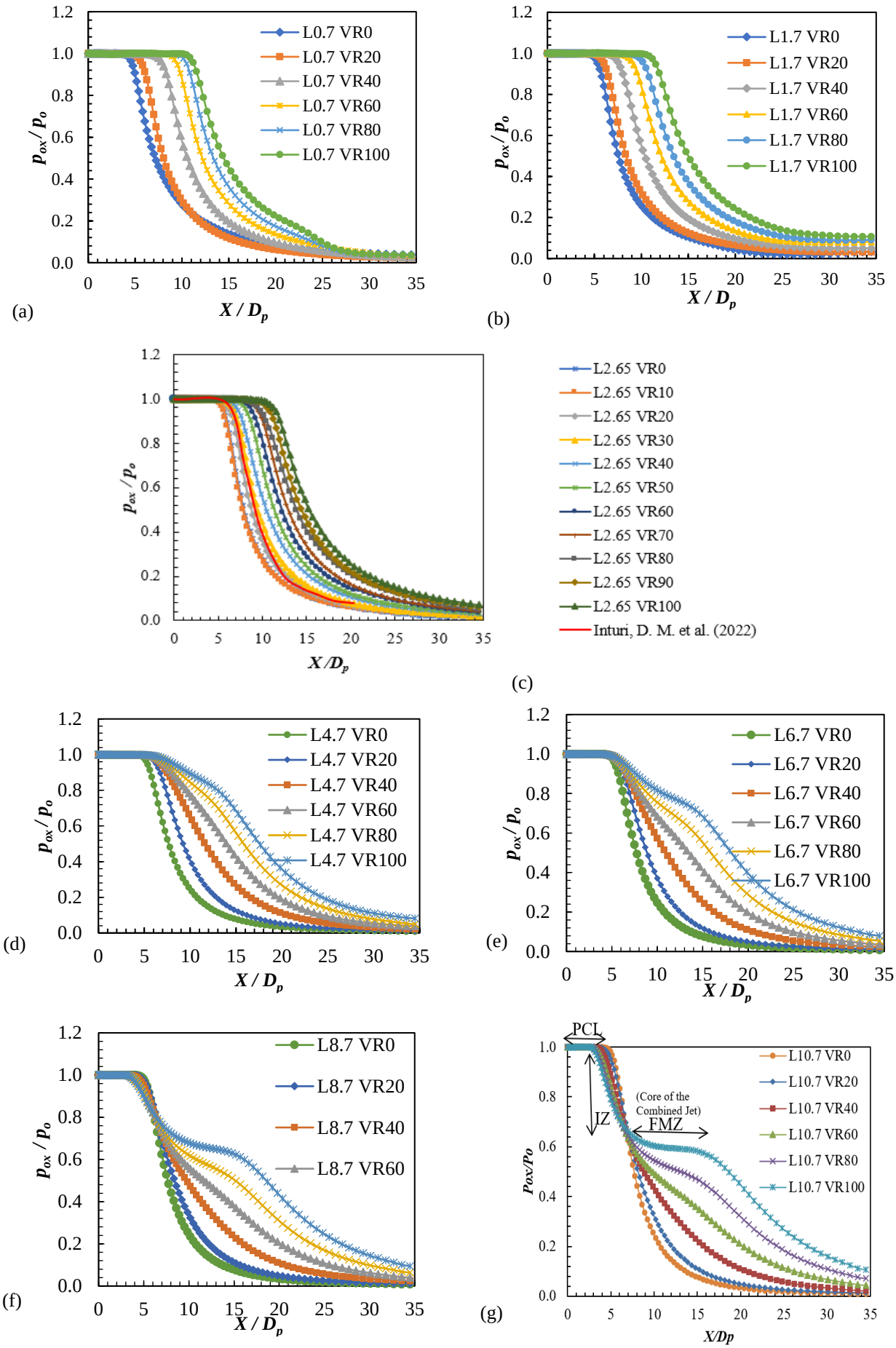

Fig. 3 Axial total pressure plot for various lip thicknesses from VR20 to VR100: (a) LT0.7mm, (b) LT1.7mm, (c) LT2.65mm, (d) LT4.7mm, (e) LT6.7mm, (f) LT8.7mm, (g) LT10.7mm

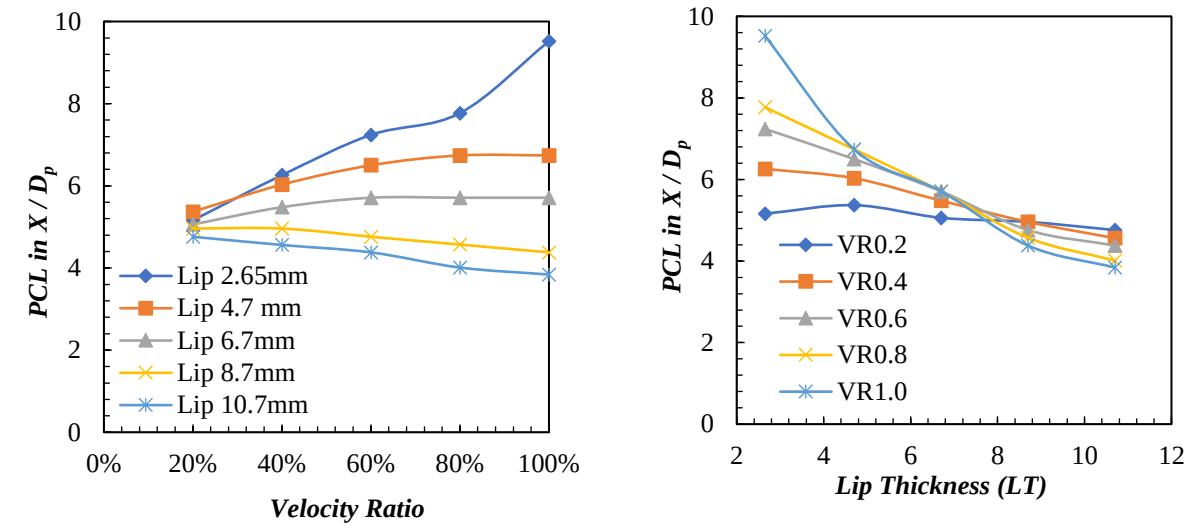

(a) (b)

Fig. 4 PCL variation with VR and LT

resulting in a less significant change in PCL with increasing VR.

Specifically, at VR20, the LT2.65mm configuration exhibits a strong shear layer, facilitating enhanced entrainment and mixing. In contrast, the LT4.7mm configuration does not exhibit any noticeable shear or wake structures under the same VR, as shown in Fig. 6(a) and discussed in Section 3.3.1. At VR100, the LT2.65mm case shows a reduction in both shear and wake dominance (Fig. 6c), resulting in a relatively extended potential core. However, in the LT4.7mm configuration, a pronounced wake region is formed, while shear layer activity remains negligible (Fig. 6c), indicating that wake-induced mixing dominates at higher VRs for this lip thickness. This is the reason for the reduction in core length from X/D_p = 9.52 (LT2.65mm) to X/D_p =5.81(LT4.7mm). As the lip thickness increases to 6.7 mm, the development of a wake region becomes increasingly pronounced at higher velocity ratios (VR). At a velocity ratio of 20% (VR20), a single, closed vortex structure is observed in the wake region, as shown in Fig. 6(a). When the velocity ratio increases to 40% (VR40), the flow field exhibits one larger closed vortex and an additional open (unclosed) vortex. Further increase in VR leads to the progressive intensification of the wake interaction between the primary and secondary jets. This behavior results in the formation of two distinct vortical structures—namely, an inner vortex and an outer vortex—clearly visible in Figs 6(b) (VR60) and 6(c) (VR100). At VR60, the outer vortex is more prominent than the inner vortex, suggesting that the wake strength is sufficient to sustain the outer structure but not dominant enough to generate a well-developed inner vortex. In contrast, at higher velocity ratios such as VR80 and VR100, the intensified wake interaction enhances the formation and clarity of both vortices, indicating a stronger shear and entrainment mechanism between the jet layers.

The potential core length of the primary jet remains nearly constant across all velocity ratios (VRs) for the lip thickness of 6.7 mm, indicating that this configuration may represent a critical lip thickness within the range investigated. Notably, the jet decay is most pronounced at VR20, as evidenced by a steeper decline in centerline velocity (Fig. 3e)). At VR100, a reduced decay slope is observed due to the early merging of the primary and secondary jets, which leads to the formation of a fully mixed zone (FMZ) shortly after the end of the interaction zone (IZ). The onset of the FMZ occurs closer to the nozzle exit for VR100 compared to other VRs, highlighting enhanced mixing and a shorter transition region. In the LT8.7mm configuration, as illustrated in Fig. 3(f), the potential core length exhibits a noticeable reduction with increasing velocity ratio (VR). This behavior is attributed to the intensified jet interaction at higher lip thickness, which significantly promotes mixing. Following this interaction, the primary and secondary jets merge to form a Fully Mixed Zone (FMZ). At VR100, the core of the combined jet becomes well-defined, indicating a strong shielding effect resulting from the unified jet structure. The velocity ratio plays a crucial role in governing the interaction between the primary jet and secondary jet, thereby influencing the decay characteristics of the primary jet.

A similar trend is observed for the LT10.7mm configuration, as shown in Fig. 3(g), where the slope of the interaction zone (IZ) progressively decreases with increasing VR.

$$\text{IWZ Slope (m)} = (y_2 - y_1) / (x_2 - x_1) \quad (2)$$

From the above relation (2) (Naren Shankar & Ganesan, 2022), it is found that for VR20, the slope is -0.12 and for VR100 the slope is -0.06. When VR increases, the slope decreases because of the shielding effect. It is understood from the slope that the shielding effect is less for low VR. For VR100 the slope is very low indicating higher shielding effect. For LT10.7mm (Fig. 3e), the percentage of core length reduction from VR20 to VR100 is not much when compared with the reduction that happened in LT2.65mm. The angle of orientation of the bending of the secondary jet is more when compared

Table 1. Initial conditions, Potential core length & Core length reduction of various LT at different VR

Primary jet exit Mach number	Primary jet exit total pressure	Primary jet Reynolds Number	Turbulence Intensity of Primary Jet	Secondary jet exit Mach number	Secondary jet exit total pressure	Secondary jet Reynolds Number	Turbulence Intensity of Secondary Jet	Velocity Ratio (VR)	Potential core length (X/D_p)						
									Lip 0.7 mm	Lip 1.7 mm	Lip 2.7 mm	Lip 4.7 mm	Lip 6.7 mm	Lip 8.7 mm	Lip 10.7 mm
0.6	1.2755	162110	4	0	0	0	0	0	4.01	4.57	4.76	4.57	4.66	4.76	4.76
				0.12	1.0100	12298	4.9305	0.2	4.96	5.16	5.16	5.37	5.06	4.38	4.19
				0.24	1.0400	24596	4.5213	0.4	6.99	6.50	6.26	5.59	4.85	4.01	3.67
				0.36	1.0936	49192	4.2979	0.6	8.61	8.05	7.24	5.59	4.85	3.84	3.34
				0.48	1.1707	36894	4.1460	0.8	9.84	9.21	7.77	5.81	4.85	3.5	3.18
				0.6	1.2755	61490	4.0319	1	10.5	10.5	9.52	5.81	4.85	3.5	3.02

with any other lip thickness of the present study. Similar to LT8.7mm, as the VR increases the flow becomes wake dominant. Increasing lip thickness reduces PCL as observed by (Srinivasarao et al., 2017) which is evident from Table 1.

3.2 Core Length Variation with VR

Figure 4 illustrates the variation in primary jet core length as a function of velocity ratio (VR) and lip thickness (LT). For lip thicknesses of LT2.65mm and LT4.7mm, an increase in VR results in a corresponding elongation of the potential core length (PCL), indicating enhanced flow stability along the jet axis. In contrast, at a thick lip thickness of 6.7 mm, the core length exhibits minimal variation with changes in VR, suggesting a transitional behavior between the primary and secondary flows. For thick lip thickness, specifically LT8.7mm and LT10.7mm, the core lengths observed across all VR conditions are significantly shorter compared to thin lip thickness configurations, indicating intensified mixing and increased momentum exchange in the near-field region. Notably, at VR100, the PCL for LT2.65 mm is significantly longer compared to other lip thickness configurations, demonstrating the strong influence of lip thickness on jet development.

3.3 Numerical Analysis

The coaxial nozzle geometry was created using the GAMBIT platform, with only the top half of the model designed due to its symmetry. A rectangular block was generated and referred to as the outlet/computational domain. The boundary conditions used are tabulated in Table 2. The model along with the computational domain is meshed for grid generation where the whole domain is discretized into small elements or cells using structured grids. At both the nozzle inlet and outlet, a fine grid is employed to accurately characterize the recirculation zone, potential core, and other essential flow properties.

The height and axial length of the domain are respectively set to be ten and forty times the measure of diameter of the principal nozzle exit. To increase the flow capture resolution, there is more grid density at the lip and coaxial nozzle exit. To achieve a fine grid near the boundary and a coarse mesh in the far field, a mesh is developed with a

Table 2 Boundary Conditions

Boundary Conditions	Regions
Wall	Primary Nozzle Wall
	Secondary Nozzle Wall
	Domain Wall
Pressure Inlet	Primary Nozzle Inlet
	Secondary Nozzle Inlet
Pressure Outlet	Primary Nozzle Outlet
	Secondary Nozzle Outlet
	Domain (top and Exit)
Axis	Primary Nozzle Axis
	Domain Axis

successive ratio of 0.9. For fine (75858), medium (52585), and coarse (28200) mesh, a grid independence study was executed (Fig. 5a).

Ansys FLUENT 6.2 solver that uses Reynolds-averaged Navier–Stokes (RANS) equation was employed for this work. Second-order upwind scheme was used for discretising the flow variables by employing implicit formulation. Boundary conditions are set on the computational domain. For a coaxial thin lip nozzle simulation, different turbulence models were compared to experimental data taken from (Lovaraju and Rathakrishnan, 2011) in order to select an appropriate turbulence model (Fig. 5b) and for thick lip (Naren Shankar & Ganesan, 2022) is used for validating the numerical results and for selecting the suitable turbulence model. The Spalart-Allmaras (SA) model was chosen after comparison with experimental data, particularly for thin and thick lip nozzles. Figs 5(b) and 5(d) demonstrate how the SA model captured centerline behavior more accurately compared to other models, justifying its use for this study.

Figure 5 (c) show different types of grids capture the flow field characteristics of thick lip in a similar manner within the jet boundary. Considering the run time and other significant parameters for analysis, the medium mesh is selected for the numerical investigations.

The effect of the grid independence research on the thin and thick lip thickness coaxial jets are shown in Fig.

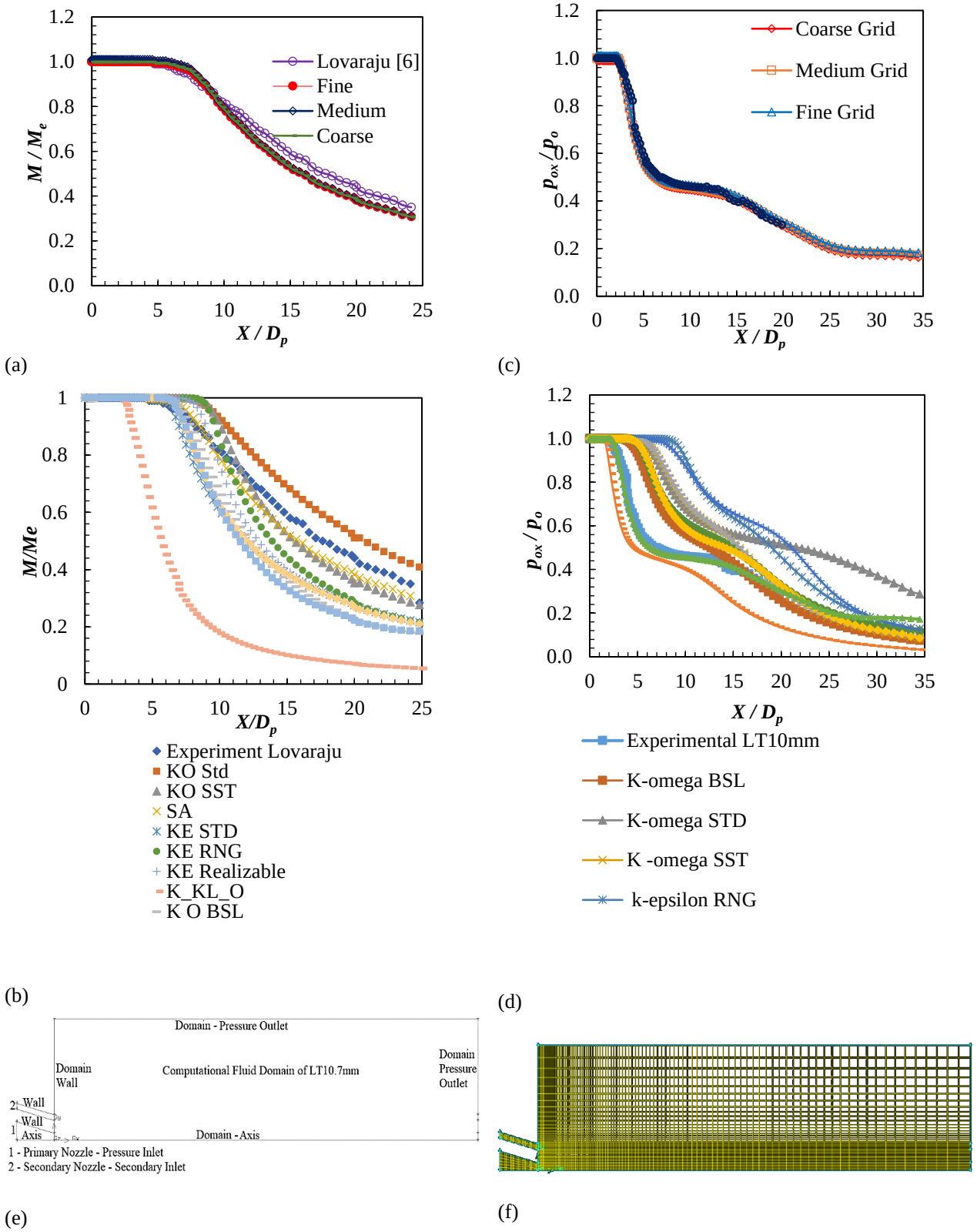

Fig. 5 (a) Grid independence study for LT2.65mm, (b) Centerline Mach number variation of different turbulence models for thin LT (LT2.65mm), (c) Grid independence study for LT10.7mm, (d) Centerline total pressure variation of different turbulence models for thick LT (LT10.7mm), (e) GAMBIT model showing coaxial nozzle along with the computational domain details, (f) Generated grid

5 (a, c). For both thin and thick lip thicknesses, the coaxial jet width remains constant at 4.4 mm, accompanied by a principal nozzle exit diameter of 11.6 mm.

The results show that the mesh point count does not influence the solution. The successive grid ratio, starting from the nozzle inlet and extending to the end of the domain, is recorded as 0.89 in both horizontal and vertical

directions. The successive ratio at the upper and lower boundaries of the domain is maintained at 1.025. Enhancing grid density near the nozzles while keeping other solution methods and parameters at default settings enhances the resolution needed to effectively capture the intricate near-field dynamics. Notably, all three grid configurations, including the coarse grid, demonstrate comparable decay characteristics along the axial centerline of the jet.

The Courant-Friedrichs-Lewy (CFL) number employed in the research varied over several thousand iterations, ranging from 0.5 to 5. The inlet served as the solution's initialization. When the solver equation finally converged after 5000 iterations, the residual value decreased by three orders of magnitude. The inlet served as the solution's initialization.

In this research, the grid error was established by using multiple grid configurations (coarse, intermediate, and fine grids). To obtain the reference value, extrapolation method, such as Richardson extrapolation (Roache, 1998), where the solutions from the coarse and fine grids were used to estimate the reference value, to assess the grid error and ensure the solution was accurate and independent of the grid size.

$$S_{ref} = S_{fine} + \frac{S_{fine} - S_{medium}}{(r^p - 1)} \quad \text{(Roache, 1998)} \quad (3)$$

$$r = \left(\frac{N_c}{N_m}\right)^{1/3} \approx \left(\frac{28200}{52585}\right)^{1/3} \approx 0.873$$

$$r^p = (0.873)^2 = 0.762$$

Based on the above equations, the S_{ref} value is 0.8786.

$$Error_f = |S_{ref} - S_f| = 0.0294$$

$$Error_m = |S_{ref} - S_m| = 0.0224$$

$$Error_c = |S_{ref} - S_c| = 0.0064$$

S_{fine} is the solution on the fine grid. S_{medium} is the solution on the medium grid. r is the successive grid ratio (0.9). p is the order of accuracy (which is usually determined empirically or from prior knowledge).

In this research, the Reynolds number (White, 2011) of the primary jet is 1.62×10^5. The secondary

jet Reynolds number vary from 0 (for a single jet or secondary jet stopped) to 6.14×10^4. The turbulence intensity (ANSYS Fluent Theory Guide, 2024) has a minimum value for a 4 and it reaches to 4.9 at maximum. When secondary jet is stopped the turbulence intensity becomes 0. The values are tabulated in Table 1.

Turbulence Intensity (TI) is given as:

$$TI = u'/U \quad (4)$$

Where, u' is the root mean square (RMS) of the fluctuating velocity component, U is the mean velocity of the flow. In turbulent pipe flow, as the Reynolds number increases, the relative magnitude of velocity fluctuations decreases slightly.

$TI \propto Re^{-n}$, where $n \approx 1/8$, thus, the turbulence intensity (TI) are calculated from an empirical formula,

$$TI = 0.16 * Re^{-1/8} \quad (5)$$

This formula is based on experimental observations of fully developed turbulent flows and is widely used in engineering practice and CFD applications to estimate inlet turbulence levels. It relates the intensity of velocity fluctuations to the Reynolds number, capturing the decreasing trend of turbulence intensity with increasing flow stability at higher Reynolds numbers.

The total pressure centerline decay plot of LT10mm from (Naren Shankar & Ganesan, 2022) has been used for validation purpose. Although the nozzle specifications and the inlet conditions are different in the present study (LT10.7mm), the decay trend and PCL is captured considerably in the Spallart Allmaras turbulence model (Fig. 5 (d)). The computational domain is shown in Fig. 5(e). The mesh figure illustrating the grid distribution, especially around the nozzle region and near boundaries, has been included in Fig. 5(f). It shows the structured mesh used in GAMBIT 2.4, with a finer grid near the nozzle and coarser in the far field to capture flow characteristics efficiently.

3.3.1 Velocity Magnitude in Pathlines

In this section, velocity contour plots of CFJs for LT2.65mm, 6.7mm and 10.7mm at VR20, VR60 and VR100 are discussed. For thin lip coaxial jets there is no wake formation (LT2.65mm). As the lip thickness increases the flow bends towards the primary jet centre axis. As the LT increases, wake region is formed between the primary jet and secondary jet and it dominantly grows as the velocity ratio increases resulting in vortex formation.

Figure 6(a) shows the velocity contour for various lip thicknesses at VR20. For the thin lip coaxial jet (LT2.65mm), there is no wake formation and it behaves as a shear-dominant flow. The low velocity coaxial jets creates an intense shear length between the primary and the secondary jet in LT2.65mm whereas in LT6.7mm and 10.7mm wake region is formed between the two jets which is clearly visible in the streamline contour. For VR20, as the LT increases, an outer vortex is formed between the near fields of the primary and secondary jets because of the recirculation region. For LT6.7mm, LT10.7mm a small completely closed outer vortex is formed. In LT10.7mm, emerging of an inner vortex can also be visualized. As the VR is increased, the recirculation zone consists of two vortices, an outer vortex and an inner vortex for LT4.7mm, LT6.7mm and 10.7mm. In VR60, the external vortex vortices are larger than those of VR20, and the inner vortex vortices are visible for LT4.7mm, LT6.7mm and LT10.7mm. For LT10.7mm, the outer vortex is closed and the inner vortex is not completely closed because of less wake dominance as evident from Fig. 6(b).

As the VR is increased to VR100 for LT4.7mm, LT6.7mm and 10.7mm both outer and inner vortex are formed completely which is evident from the vortices visible in Fig. 6(c). Outer vortex is the reason for the formation of inner vortex. Both vortices are formed due to the wake dominance. The flow originating from the outer vortex (near secondary jet) of the recirculation vortex is

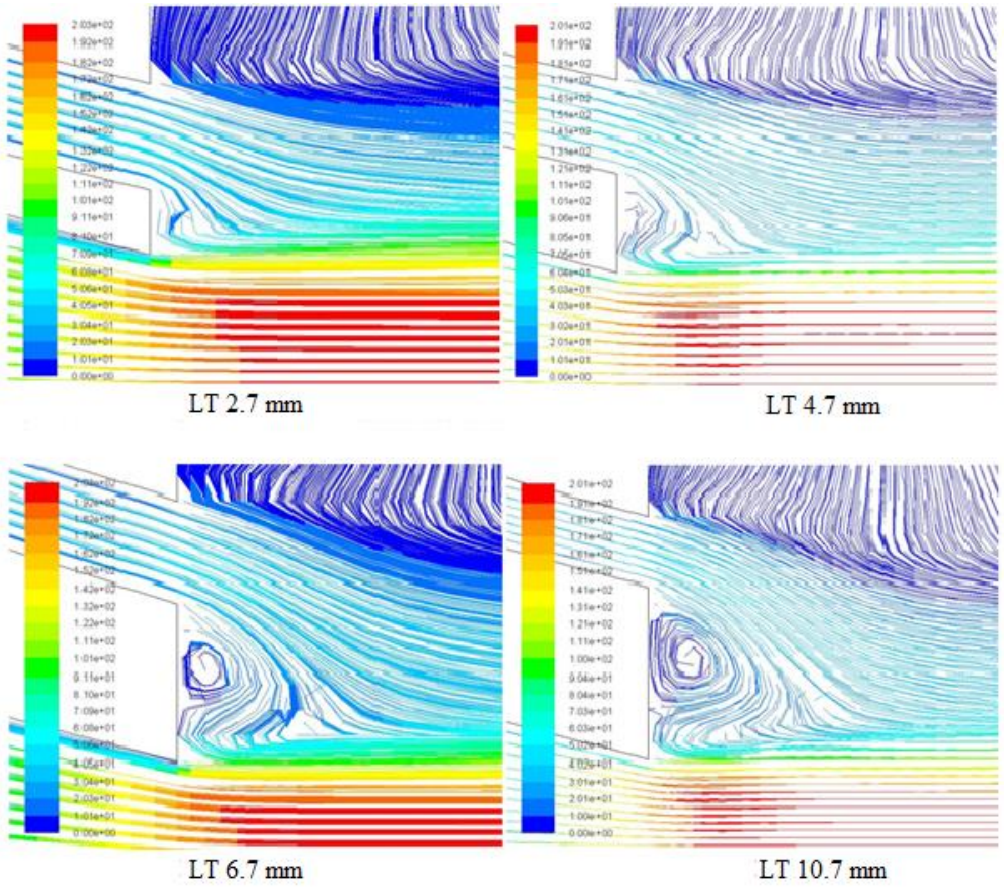
LT 2.7 mm
LT 4.7 mm
LT 6.7 mm
LT 10.7 mm

(a)

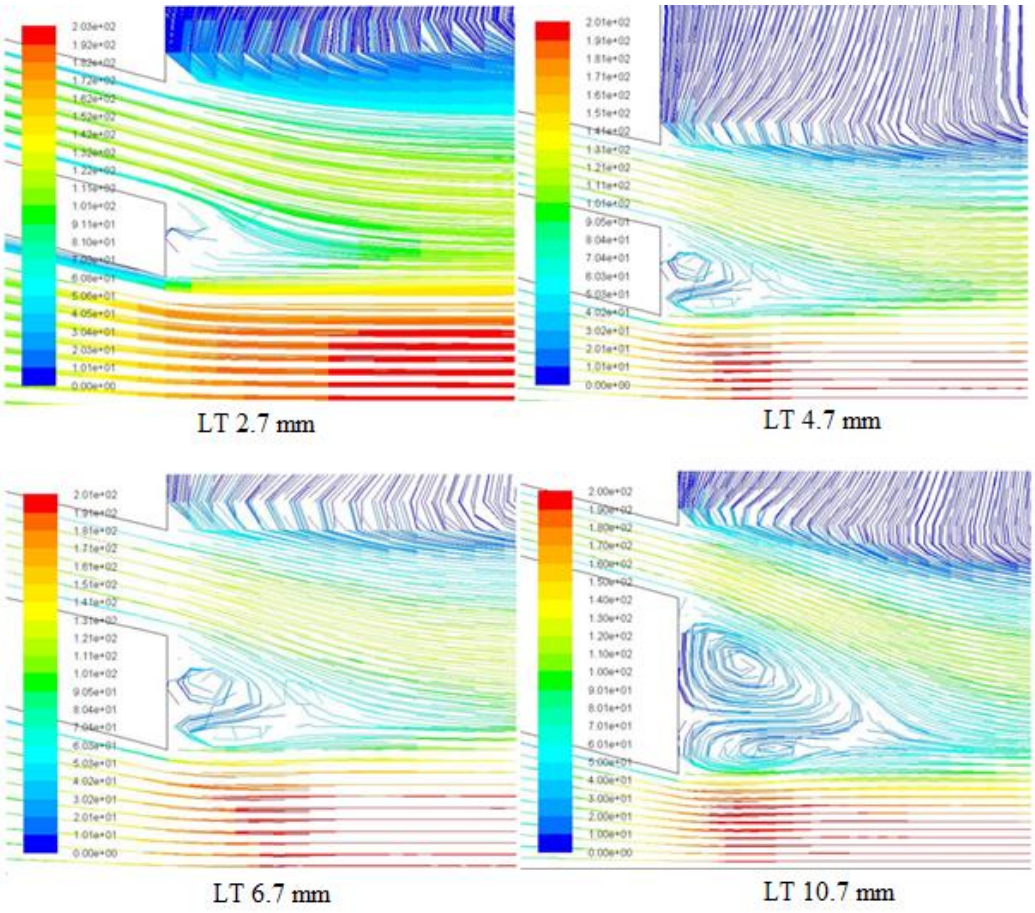
LT 2.7 mm
LT 4.7 mm
LT 6.7 mm
LT 10.7 mm

(b)

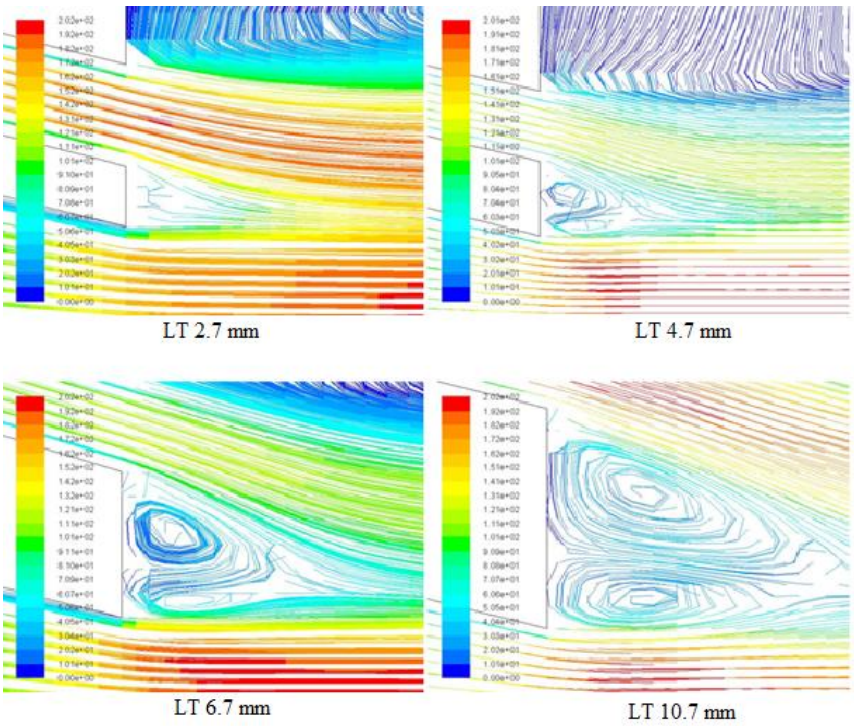

(c)

Fig. 6 Streamline contour for various lip thickness: (a) VR20, (b) VR60, (c) VR100

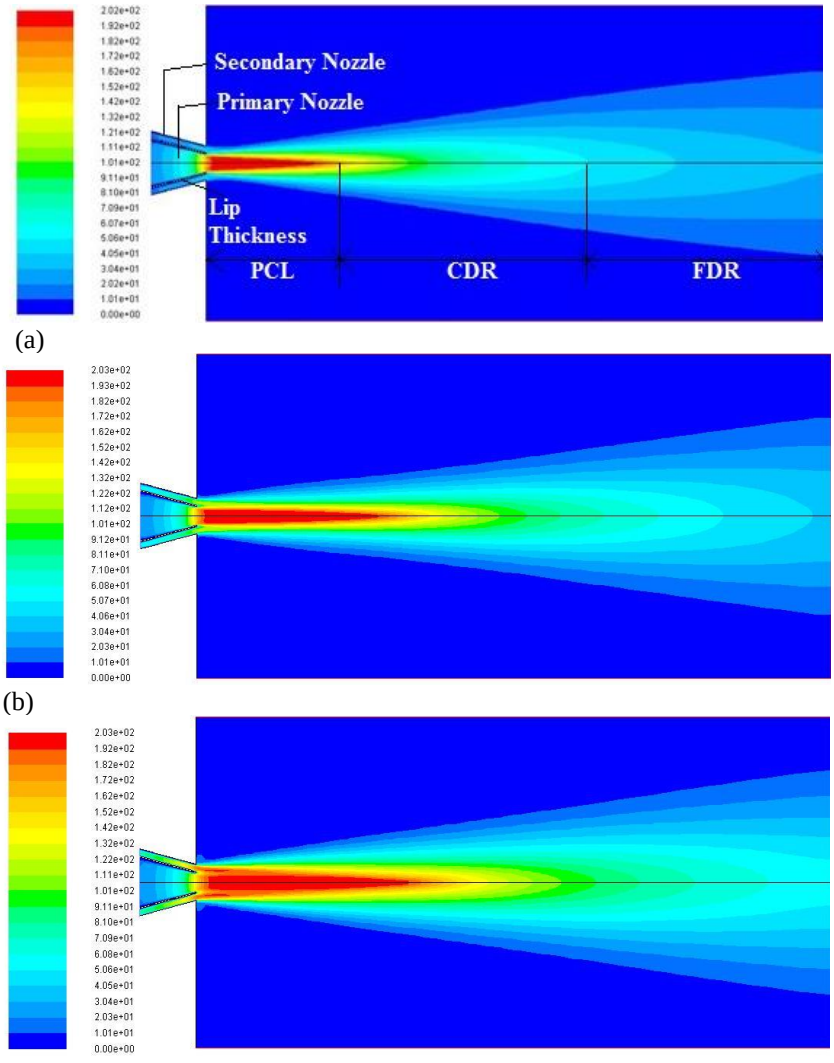

(a)

(b)

(c)

Fig. 7 Velocity Contours for LT0.7mm : (a) VR20 (b) VR60 (c) VR100

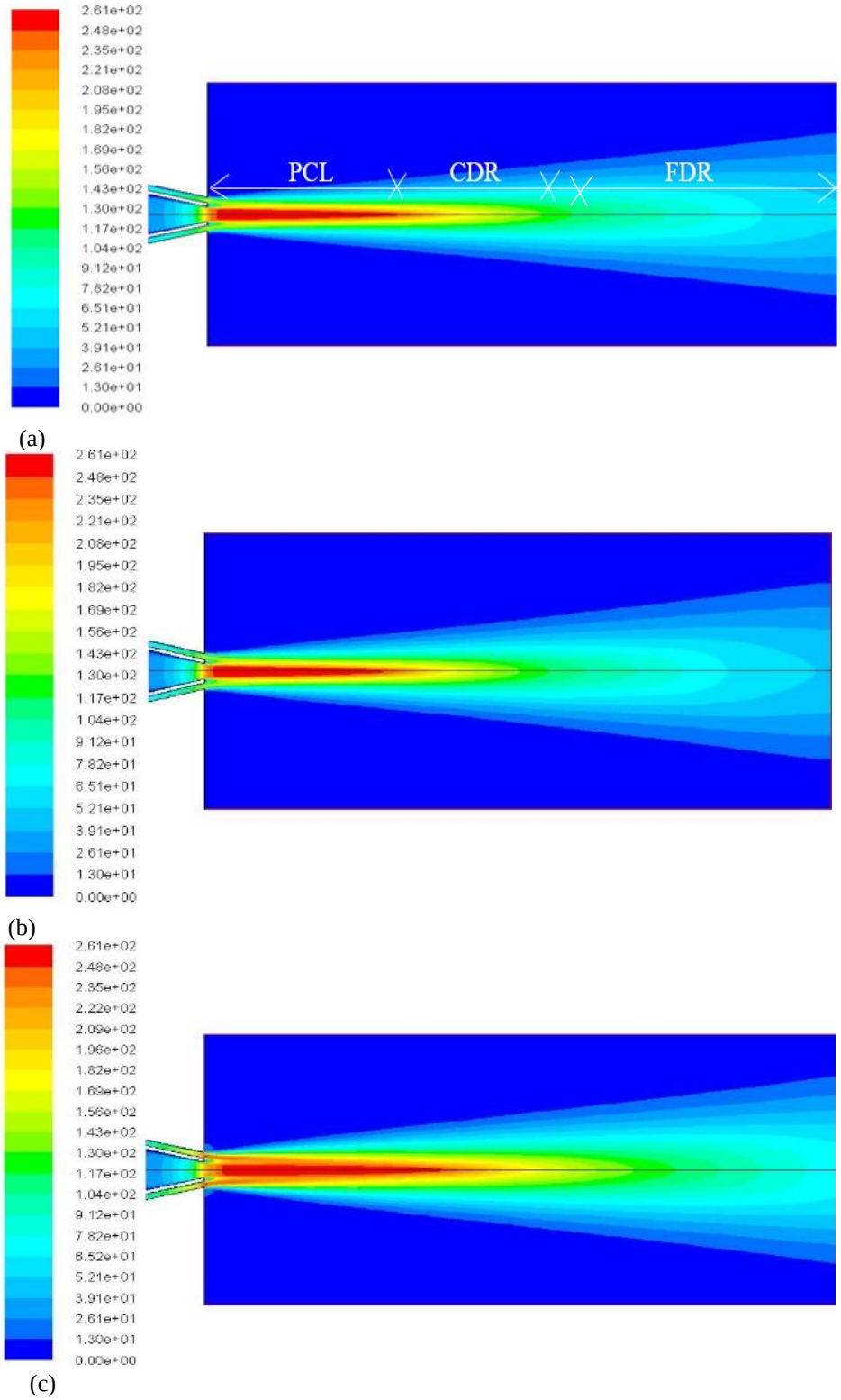

Fig. 8 Velocity Contours for LT2.65mm : (a) VR20, (b) VR60, (c) VR100

transferred towards the inner jet forming the inner vortex if the wake is dominant, resulting in a net mass flow across the axis of symmetry. The two vortices formed because of recirculation vortex are not in the same size (Taglia et al., 2004). At low VR, the formation of a vortex/recirculation zone is hindered. For LT2.65mm the core length for VR100 is X/Dp=9.52 whereas for LT10.7 the core is drastically reduced to X/Dp=3.02 which is nearly 8% of the core reduction (Table 1). This reduction is because of the significant influence of the wake flow as LT is increased.

3.3.2 Velocity Contours for Varying Lip Coaxial Jets

There is a correlation between the primary potential core length and the velocity ratio when the lip thickness increases. Velocity contour graphics for coaxial jets are illustrated in this section for thin (LT0.7mm, LT2.65mm) and thick lip thickness (LT8.7mm, LT10.7mm), with the

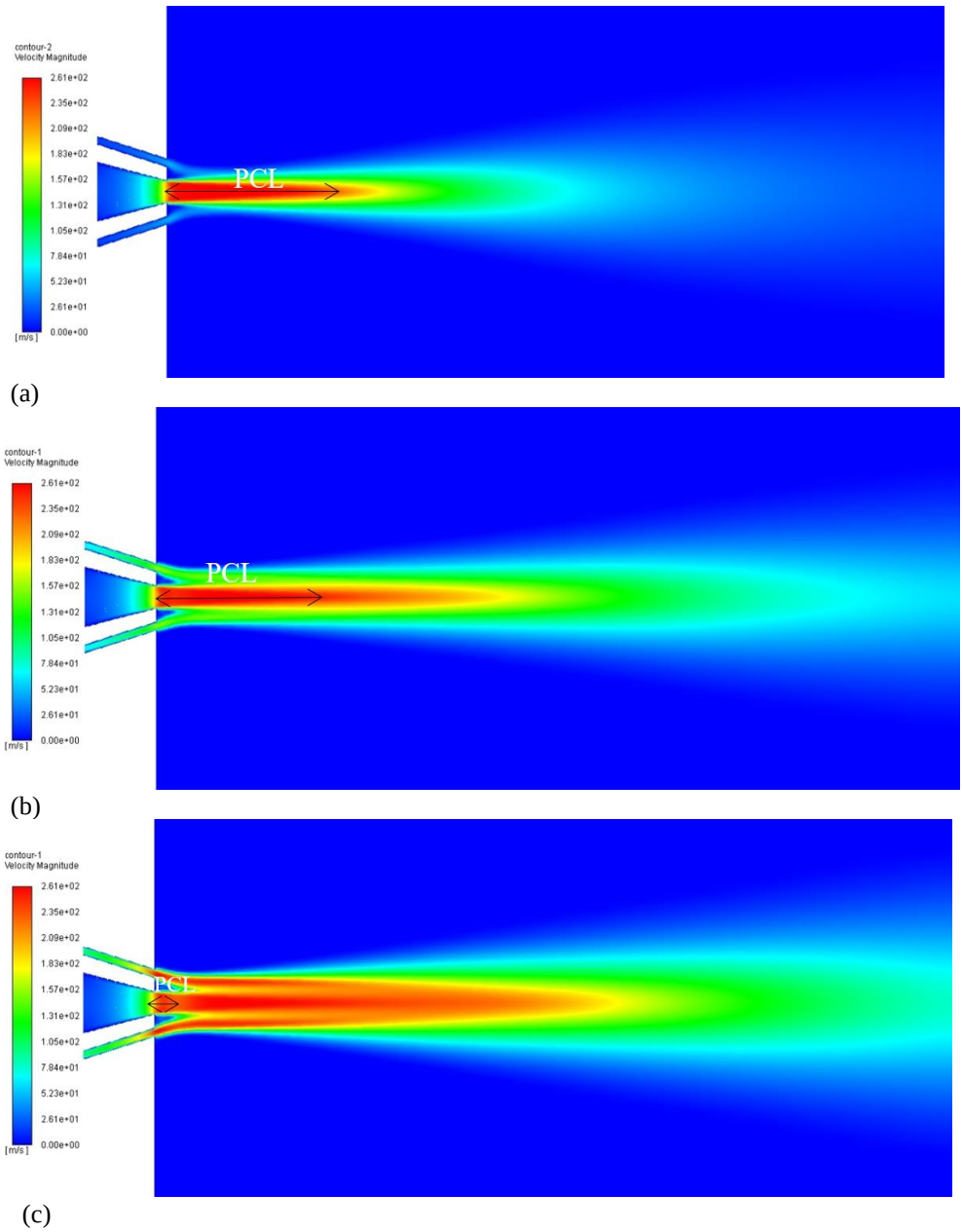

Fig. 9 Velocity Contours for LT8.7mm : (a) VR20, (b) VR60, (c) VR100

contours displayed in Fig. 7, 8, 9 and 10 correspondingly. The potential core length of the coaxial jet is visible from the velocity contour, with velocity magnitudes depicted in the legends positioned on the LHS of the contour plots, measured in meters per second. The jet flow characteristics include three primary segments - PCL, CDR, and FDR, which collectively characterize the flow, as demonstrated in Fig. 7-10.

In thin lip case (LT0.7mm (Fig. 7), LT2.65mm (Fig. 8)) VR20 was found to have a shorter core and a fast decrease in the Pitot pressure when compared to the other VRs. Compared with the VR60, VR80, and VR100 jets, VR20 and VR40 jets provide better mixing in the core zone, as shown by a smaller core size, and characteristic zone. It is more likely that shearing will occur at low velocity ratios. In this way, the entrainment between the primary jet and the secondary jet is improved, which shortens the core length. Additionally, it is seen from the figure that the consistent width of velocity along the potential core for a velocity ratio of 100 is considerably broader along the stream axial centreline in contrast to a velocity ratio of 20. The rise in velocity ratio results in an extended potential core length. Furthermore, Figure 7 (LT0.7mm) and 8 (LT2.65mm) also highlights the substantial increase of the primary jet core as the velocity ratio increases.

In LT2.65mm, VR20, the primary core length reduces compared to VR 60 and 100 in the nearfield, as depicted in Fig. 8(a-c). Furthermore, secondary core is not visible for both LT0.7mm (Fig. 7(a-c)) and LT2.65mm (Fig. 8(a-c)). This lack of visibility is due to the dominant primary shear layer, which draws the secondary jet towards the primary jet, thus increasing the mixing. With rising VR, more shielding is generated between the secondary and primary jet, resulting in reduced entrainment, and mixing. Conversely, the presence of the main shear layer, which is less significant, inhibits mixing. At VR 20, the shielding

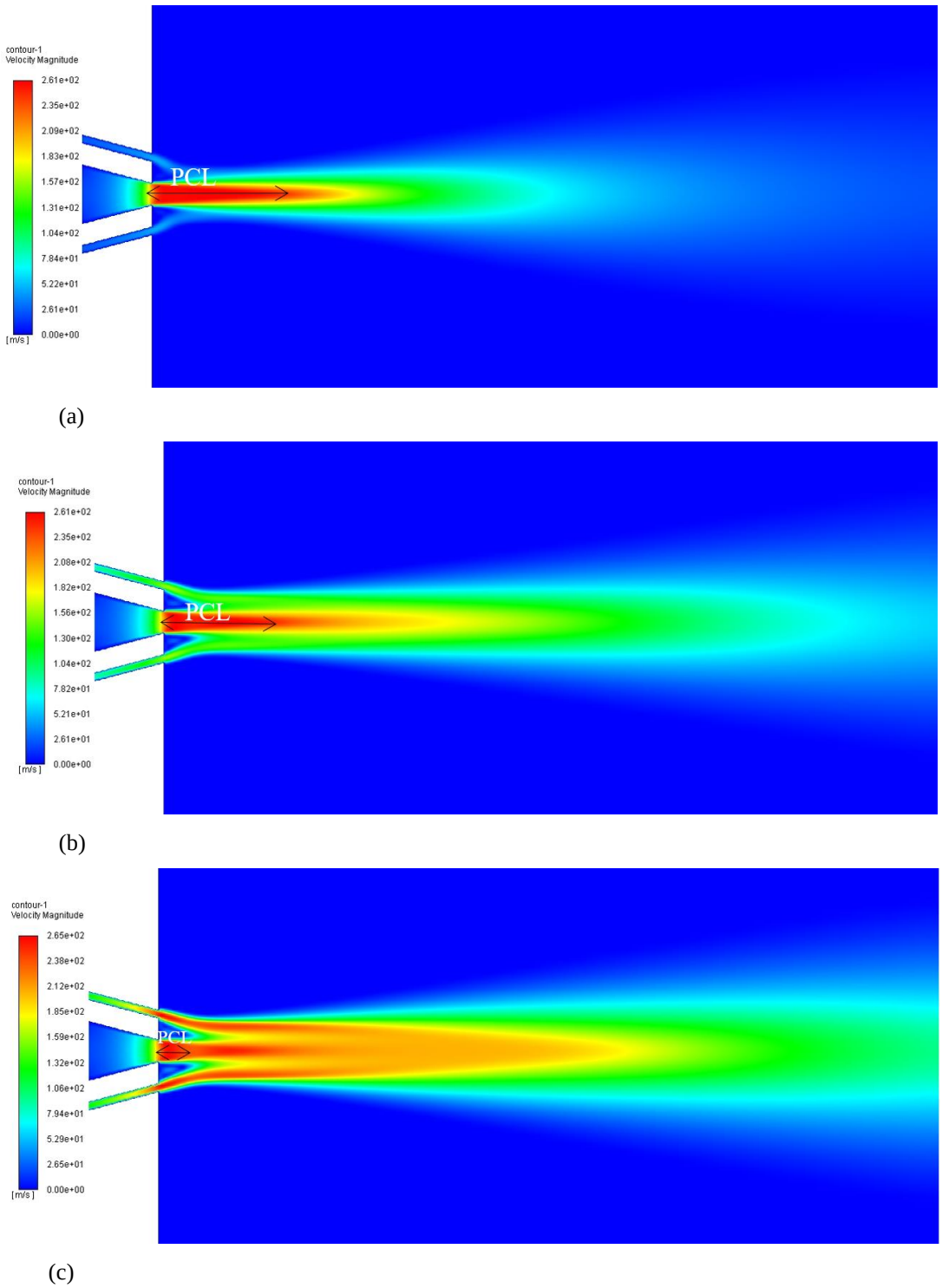

Fig. 10 Velocity Contours for LT10.7mm : (a) VR20, (b) VR60, (c) VR100

effect is not significant, leading to greater entrainment and consequently a shorter core extent.

In VR60, as depicted in Fig. 7(b) and 8(b), the secondary jet shields the primary jet, thereby inhibiting its interaction with the surrounding stagnant atmosphere. The magnitude of the primary shear layer decreases as VR increases. Consequently, since the primary shear layer of VR60 is less dominant compared to VR20 (Fig. 7(a) and 8(a)), there is reduced entrainment between the primary and secondary jets.

The prevailing shielding effect between the secondary and primary jets develops prominently for VR100, as illustrated in Fig. 7(c) and Fig. 8(c), leading to an increase in the primary jet core length. Moreover, it is seen that in coaxial jets with high VR, the primary and secondary jets merge to create a FMZ at the far-off end of the primary jet's axial range.

The velocity contours of thin lip jets (Figs 7(a-c) and 8(a-c)) clearly show no vortex or wake formation near the nozzle exit, as confirmed in Sections 3.3.1. This similar

trend is observed for LT4.7mm which is evident from Table 1.

In contrast, increasing lip thickness leads to wake formation at the nozzle near field (Fig. 9 and 10). In thick lip for LT8.7mm (Fig. 9) and LT10.7mm (Fig. 10), when increasing the VR, a notable reduction in the core is observed.

Velocity Contours for thick lip thickness are visually represented in Fig. 9(a-c) and Fig. 10(a-c). Here, although the red regions appear elongated, the full dark red region does not accurately reflect the actual size of the constant velocity region. In fact, a comparative assessment of Fig. 4.18 (a-c) reveals that, despite the perceived elongation, the effective core extent is diminishing as VR increases. This is indicated by a dark red shade in the figures which denote the extent of the core; once the flow moves beyond this, the velocity begins to dissipate. This dissipation is clearly specified by the accompanying velocity legends in Fig. 9(a-c).

Furthermore, this trend is consistently mirrored in the analysis of LT10.7mm (Fig. 10(a-c)).

4. CONCLUSION

Experimental studies of a coaxial jet with varying velocity ratio at various lip thickness of 0.7mm, 1.7mm, 2.65mm, 4.7mm, 6.7mm, 8.7mm and 10.7mm are presented in this paper. The secondary jet with varying velocities (VR20, VR40, VR60, VR80 and VR100) is fed into a constant primary jet velocity of Mach 0.6. The following conclusions are made from the present study.

1. At thin lip thickness (LT 0.7mm, 1.7mm, 2.65mm), as the velocity ratio is increased, there is an predominant increase in the potential core length. At thick lip thickness, as the velocity ratio increases, the potential core length decreases predominantly (LT8.7mm and LT10.7mm).
2. At critical lip thickness (LT6.7mm), the core length remains almost constant even with an increase in the velocity ratio.
3. The velocity ratio of coaxial jet has strong influence on the jet mixing. Thin lip coaxial jet (lip 0.7mm, lip 1.7mm, lip 2.65mm and lip 4.7mm) with VR20 and VR40 experience a significantly higher mixing than VR60, VR80 and VR100 jets. For higher lip thickness values (lip 8.7mm and lip 10.7mm), the mixing of VR20 and VR40jets become inferior to that of VR60, VR80 and VR100 jets.
4. For low velocity ratio, as the lip thickness is increased, there is not much reduction in the potential core length. The core length value for VR20, LT2.65mm is X/D_p=5.16, while the core for VR20, LT10.7mm is X/D_p=4.2mm, which gives a potential core reduction of 1.4.
5. As the velocity ratio is increased, increasing the lip thickness leads to a drastic reduction in the potential core length. For VR100, LT2.65mm the core length is X/D_p=9.52 while for VR100, LT10.7mm the core length is X/D_p=3.02.
6. For LT2.65mm, increasing the velocity ratio has no effect in formation of vortices between the two jets whereas for LT4.7mm, at low velocity ratio (VR20) there is no vortex formed in between two jet. When the velocity ratio is increased formation of vortex between primary and secondary jets in the near field is visible which makes the flow to be wake dominant.
7. At low velocity ratio (VR20), as the lip thickness is increased, one closed vortex (outer vortex) and one unclosed vortex (inner vortex) are formed. Thus, it is concluded that the mixing due to the effect of lip for VR20 is marginal (for LT2.65mm, PCL=5.16 D_p, for LT10.7mm, PCL = X/D_p=4.19 D_p).
8. At VR40, VR60 for lip thicknesses 4.7mm, 6.7mm, 8.7mm and 10.7mm, the outer closed vortex and inner unclosed vortex grows to be dominant. Lip 2.65mm has no possibility of vortex/recirculation zone formation because of thin lip.
9. At thick lip thicknesses (LT 8.7mm and LT10.7mm), and at VR80, VR100 two closed vortices are formed. The vortex dominance is the reason for the core reduction.
10. Core of the thin lip with VR100 (for LT2.65mm, core is X/D_p=9.52) is 64.5% longer than the core length of thick lip (for LT10.7mm, core is X/D_p=3.84). It is concluded that the mixing due to the effect of lip for VR100 is dominant.

As a potential extension of this work, future studies will investigate the effects of varying the thermal ratio on the behavior and mixing characteristics of subsonic coaxial jets.

ACKNOWLEDGEMENTS

The authors sincerely acknowledge the Department of Science and Technology, Science and Engineering Research Board (DST-SERB), Government of India, for funding this research on coaxial jets through the TARE scheme (Grant No. TAR/2021/000093). The authors also gratefully acknowledge the financial support received from Vel Tech Rangarajan Dr. Sagunthala R&D Institute of Science and Technology, under the Research Development Fund (RDF), Grant No. VTU/RDF/FY 2025-26/042. This support was instrumental in facilitating the successful execution of this research work.

CONFLICT OF INTEREST

The authors wish to confirm that there are no known conflicts of interest associated with this publication and there has been no significant financial support for this work that could have influenced its outcome.

AUTHORS CONTRIBUTION

Irish Angelin: Conceptualization, Methodology, Investigation, Writing – Original Draft. **R. Naren Shankar:** Conceptualization, Methodology, Supervision. **K. Sathish Kumar:** Methodology, Investigation, Review and Editing. **K. Anusindhiya:** Review and Editing. **K. Vijayaraja:** Supervision. **E. Rathakrishnan:** Supervision.

REFERENCES

ANSYS Fluent Theory Guide (2024) *Turbulence Intensity*, *ANSYS*.

Buresti, G., Talamelli, A., & Petagna, P. (1994). Experimental characterization of the velocity field of a coaxial jet configuration. *Experimental Thermal and Fluid Science*, *9*(2), 135–146, https://doi.org/10.1016/0894-1777(94)90106-6.

Champagne, F. H., & Wygnanski, I. J. (1971). An experimental investigation of coaxial turbulent jets. *International Journal of Heat and Mass Transfer*, *14*(9), 1445–1464. https://doi.org/10.1016/0017-9310(71)90191-8.

Chigier, N. A. & Beer, J. M. (1964). The flow region near the nozzle in double concentric jets. *Journal of Basic Engineering*, *86*, 797–804, https://doi.org/10.1115/1.3655957.

Dahm, W. J., Frieler, C. E., & Tryggvason, G. (1992). Vortex structure and dynamics in the near field of a coaxial jet. *Journal of Fluid Mechanics*, *241*(32), 371–402. https://doi.org/10.1017/S0022112092002088.

Hewes, A., & Mydlarski, L. (2023). Multi-scalar mixing in turbulent coaxial jets. *Journal of Fluid Mechanics*, *961*, 1–42. https://doi.org/10.1017/jfm.2023.218.

Inturi, D. M., Lovaraju, P., Tanneeru, S. R., & Rathakrishnan, E. (2022). Effect of eccentricity on co-flow jet characteristics. *Iranian Journal of Science and Technology, Transactions of Mechanical Engineering*, *46*(2), 407–420. https://doi.org/10.1007/s40997-021-00444-2.

Ko, N. W. M., & Kwan, A. S. H. (1976). The initial region of subsonic coaxial jets. *Journal of Fluid Mechanics*, *73*(2), 305–332. https://doi.org/10.1017/S0022112077000664.

Kwan, A. S. H., & Ko, N. W. M. (1976). Coherent structures in subsonic coaxial jets. *Journal of Sound and Vibration*, *48*(2), 203–219. https://doi.org/10.1016/0022-460X(76)90460-0.

Lovaraju, P., & Rathakrishnan, E. (2011). Experimental studies on co-flowing subsonic and sonic jets. *Flow, Turbulence and Combustion*, *87*(1), 115–132. https://doi.org/10.1007/s10494-011-9332-5.

Naren Shankar, R., & Ganesan, V. G. (2022). Experimental and numerical studies of co-flowing jets with finite lip thickness and varying bypass ratio. *Advances in Materials and Processing Technologies*, *00*(00), 1–25. https://doi.org/10.1080/2374068X.2022.2076987.

Naren Shankar, R., Kevin Bennett, S., & Dilip Raja, N. S. K. K. (2020). Characteristics of a co-flowing jet with varying lip thickness and constant velocity ratio. *Aircraft Engineering and Aerospace Technology*, *92*(4), 633–644. https://doi.org/10.1108/AEAT-05-2019-0104.

Naren Shankar, R., Thanigaiarasu, S., Elangovan, S., & Rathakrishnan, E. (2021). Co-flowing jet control using lip thickness variation. *International Journal of Turbo & Jet-Engines*, *38*(3), 289–302. https://doi.org/doi:10.1515/tjj-2018-0024.

Georgiadis N., & Papamoschou. (2003). Computational investigations of high-speed dual-stream jets. *In 9th AIAA/CEAS Aeroacoustics Conference and Exhibit (p. 3311).* https://doi.org/10.2514/6.2003-3311.

Orlu, R., Segalini, A., Alfredsson, P. H., & Talamelli, A. (2006). *Passive control of mixing in a coaxial jet*. Proc. 7th Int. ERCOFTAC Symp. on Engineering Turbulence Modelling and Measurements, pp. 450–455.

Orlu, R., Segalini, A., Alfredsson, P., & Talamelli, A. (2008). *On the passive control of the near-field of coaxial jets by means of vortex shedding*. Proceedings of Internatioanl Conference on Jets, Wakes and Separated Flows, Technical University of Berlin, Germany, pp.1-7.

Rathakrishnan, E. (2009). Experimental studies on the limiting tab. *AIAA Journal*, *47*(10), 2475–2485. https://doi.org/ 10.2514/1.43790.

Roache, P. J. (1998). *Verification and validation in computational science and engineering*, Hermosa Publishers., New Mexico, USA.

Segalini, A., & Talamelli, A. (2011). Experimental analysis of dominant instabilities in coaxial jets. *Physics of Fluids*, *23*(2). https://doi.org/10.1063/1.3553280.

Srinivasarao, T., Lovaraju, P., & Rathakrishnan, E. (2014a). Characteristics of co-flow jets from orifices. *International Journal of Turbo & Jet-Engines*, *31*(2), 141–148. https://doi.org/10.1515/tjj-2013-0040.

Srinivasarao, T., Lovaraju, P., & Rathakrishnan, E. (2014b). Characteristics of underexpanded co-flow jets. *Applied Mechanics and Materials*, 575(August), 507–511. https://doi.org/10.4028/www.scientific.net/AMM.575.507.

Srinivasarao, T., Murthy, I. D., Lovaraju, P., & Rathakrishnan, E. (2017). Effect of inner nozzle lip thickness on co-flow jet characteristics. *International Journal of Turbo & Jet-Engines*, *34*(3), 287–293. https://doi.org/10.1515/tjj-2016-0004.

Taglia, C. T., Blum, L., Gass, J., Ventikos, Y., & Poulikakos, D. (2004). Numerical and experimental investigation of an annular jet flow with large

blockage. *Journal of Fluids Engineering, Transactions of the ASME*, *126*(3), 375–384. https://doi.org/10.1115/1.1760533.

White, F. M. (2011). *Fluid Mechanics*. 7th edn. New York, NY, USA: McGraw-Hill. https://doi.org/10.13140/RG.2.2.21339.62244.

Zaman, K. B. M. Q., & Dahl, M. D. (2007). Noise and spreading of subsonic coannular jets — comparison with single equivalent jet. *AIAA Journal*, *45*(11), 2661–2670. https://doi.org/10.2514/1.29441.